ADV MATH SCI JOURNAL
Advances in Mathematics: Scientific Journal **9** (2020), no.10, 8153–8163
ISSN: 1857-8365 (printed); 1857-8438 (electronic)
https://doi.org/10.37418/amsj.9.10.45 Spec. Iss. on AOAOCEP-2020

APPLICATION OF SOLAR PHOTOVOLTAIC AND STATCOM FOR POWER SYSTEM OSCILLATION DAMPING AND STABILITY IMPROVEMENT

L.V. SURESH KUMAR[1], D.V.N. ANANTH, M. PREMKUMAR, AND RAVIPUDI SUDHIR

ABSTRACT. The power system will function effectively till a disturbance like fault or load changes or source side issues took place. These disturbances depending on amplitude and time will influence the power system parameters behavior. If a severe low voltage fault occurs for short period influences lesser than for a longer period for the same system. So, in this analysis, behavior of a power system containing conventional synchronous generator system, solar photovoltaic system and a STATCOM are all considered as a unit and the system is connected to a faulty weak grid. The overall system oscillations damping and stability are observed without observer, with fuzzy-controller (FC) and with H-∞ controller (HC). The MATLAB/Simulink is used for the study and HC observed to be performing superior than FC incorporated system.

1. INTRODUCTION

The power system has various sources, transmission and distribution network and load centers. For improving the load profile, along with the conventional source containing synchronous generators, the renewable energy resources like wind, solar, FACTS devices like STATCOM and energy storage devices like battery, fuel-cell, ultra capacitors are helpful [1–3]. These sources and devices help in damping oscillation of voltage, frequency, power rotor speed and other important parameters in the power system, thereby this load profile is improved. To take care of high disturbance, the additional renewable energy resources,

[1]*corresponding author*
2020 *Mathematics Subject Classification.* 34C55, 93B36, 93C42.
Key words and phrases. Damping, fuzzy controller, H-∞, photovoltaic (PV), stability, STATCOM.

and FACTS devices will be very helpful in power oscillations and voltage oscillations damping and frequency improvement [4]. TFew FACTS devices like STATCOM, UPFC, SVC, TCSC and energy storage devices like SMES, batteries, super-capacitors if used with these renewable energy resources will improve overall system stability [5, 6]. The power oscillations damping with solar PV-STATCOM etc are studied by many authors and sound that renewable energies and FACTS devices will definitely improve the power oscillations damping and overall stability [7].

Few authors observed the power oscillations damping is effective when advanced robust controllers like H-infinity (H∞) controllers, fuzzy controllers, neural networks, meta-heuristic multi-objective controllers will be very helpful [8, 9]. These robust controllers will be faster, accurate and lesser parameter dependent and act according to the system and its fault behavior. In this paper, solar PV source, STATCOM are used to aid the power oscillations damping and stability improvement. For further quicker and accurate controller action, H-infinity (H∞) controllers (HC) and fuzzy controllers (FC) are used for the same system to find the effective controller among these two. The MATLAB software is used to observe the behavior when a large sudden disturbance is occurred at the grid load point the system parameters behavior is studied.

The Section-II describes the test system under study. Section-III discusses the H∞ controller block diagram used in this paper. Section-IV analyzes the system results without any controller with its internal PSS, and with H∞ and fuzzy controllers. The conclusion drawn is shown in Section-V.

2. Test System Under Study

In this paper, a single machine infinite bus system is considered for the analysis as shown in Fig.(1) The impedance in the transmission line is represented with an inductance of X_{12} ohms, with voltage and angle in area-1 is V_1 and δ_1 and at the grid is V_1 and δ_2 respectively at the buses 1 and 2. The internal view of the area-1 is shown in Fig.1b, which contains conventional generator having synchronous generator, a STATCOM and a solar PV cell and its internal load.

2.1. **Solar PV panels and inverter unit:** The solar PV panel system with inverter unit simplified block diagram is shown in Fig.2(a). There will be a source

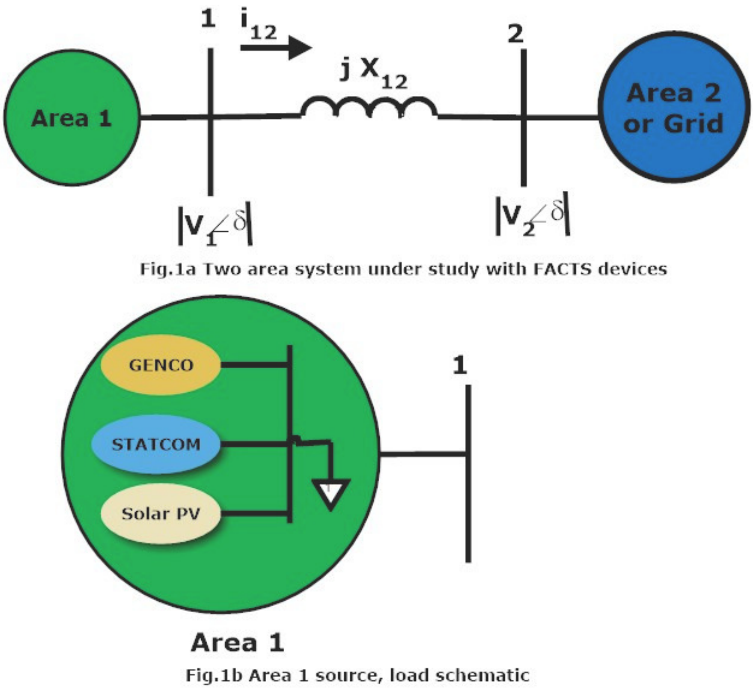

FIGURE 1. Test system for the study

side inductor for current smoothening and then a switch in parallel for chopping or regulating dc voltage application to a constant voltage irrespective of irradiance. Then capacitors are used to supply constant voltage to the inverter switches even with large load or grid disturbances. The filter bank contains LCL elements to improve the voltage and current waveforms to the grid requirements. The current-voltage (I-V) and power-voltage (P-V) characteristics of the solar panel at different irradiance values is shown in Fig.2(b) and Fig.2(c).

2.2. **STATCOM controller.** The STATCOM is treated as current injecting device and the block diagram is shown in Fig.3(a) [10].

$$\frac{dI_{std}}{dt} = \frac{-\omega_s R_{st}}{X_{st}} I_{std} + \omega_s I_{stq} - \omega_s \frac{\sin(\alpha+\theta_s)}{X_{st}} V_{dc} + \frac{\omega_s}{X_{st}} \cos(\theta_s) V_s \tag{2.1}$$

$$\frac{dI_{stq}}{dt} = \frac{-\omega_s R_{st}}{X_{st}} I_{stq} + \omega_s I_{std} - \omega_s \frac{\cos(\alpha+\theta_s)}{X_{st}} V_{dc} + \frac{\omega_s}{X_{st}} \sin(\theta_s) V_s \tag{2.2}$$

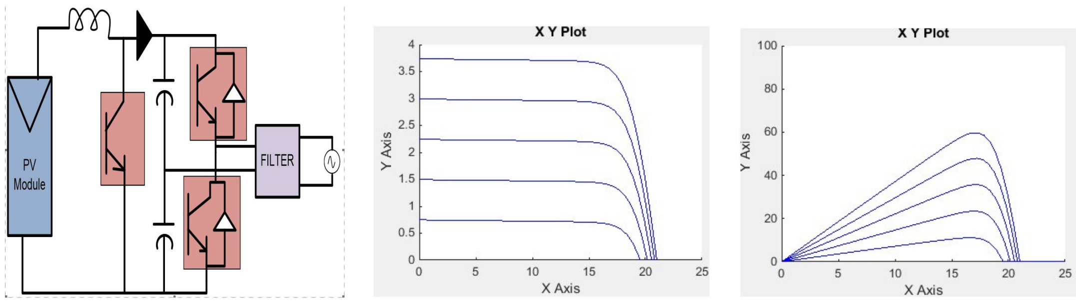

(a) Solar PV inverter (b) I-V characteristics (c) P-V characteristics

FIGURE 2. Solar PV system

The d and q axis STATCOM current injection equations are shown in equations (2.1) and (2.2), with system natural angular frequency (ω_s), resistance (R_{st}) and inductance(X_{st}), voltage (V_s) and dc link voltage (V_{dc}) across the capacitor. The positive sign of the current flow indicates the current flow to the mid-point from the STATCOM, acting like current injection (capacitor behaviour) and negative current direction indicates,the STATCOM capacitor is receiving the current and making it to charge as an absorbing property or lagging power factor (inductor behaviour) load. The dynamic DC link capacitor voltage by the STATCOM is given by

$$\frac{dV_{dc}}{dt} = -\sqrt{3}\omega_s X_{dc}(I_{std}\sin(\alpha+\theta_s) + I_{stq}\cos(\alpha+\theta_s)) \tag{2.3}$$

The STATCOM real and reactive power flow rating can be decided based on STATCOM and source voltage ratings as

$$P_{st} + jQ_{st} = \frac{V_s V_{st} e^{-j\alpha} - V_s^2}{R_{st} - jX_{st}}. \tag{2.4}$$

By expanding the imaginary exponential parameter and separating real and imaginary parts of the equation (2.4), we get the equation (2.5) describing the real power flow and equation (2.6), the reactive power flow.

$$P_{st} = \frac{V_s V_{dc} R_{st}\cos\alpha + V_s V_{dc} X_{st}\sin\alpha - R_{st}V_s^2}{R_{st}^2 + X_{st}^2}. \tag{2.5}$$

$$Q_{st} = \frac{V_s V_{dc} X_{st}\cos\alpha - V_s V_{dc} R_{st}\sin\alpha - X_{st}V_s^2}{R_{st}^2 + X_{st}^2} \tag{2.6}$$

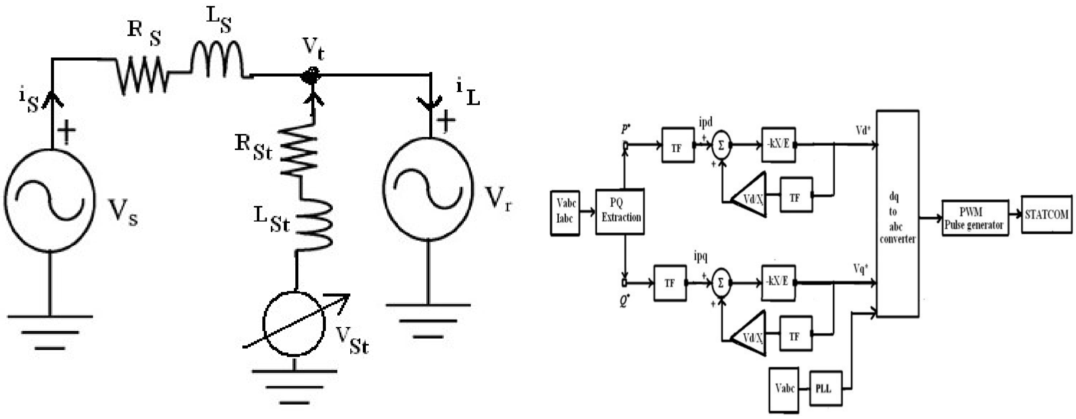

(a) Single line diagram (b) STATCOM-PWM switching

FIGURE 3. STATCOM controller

The STATCOM d and q axis current flow described in the equations (2.1) and (2.2) are simplified with the operation under the steady- state and rewritten as in equations (2.7) and (2.8) as

$$\frac{dI_{std}}{dt} = \frac{-R_{st}}{L_{st}} I_{std} + \omega_s I_{stq} + \frac{1}{L_{st}}(V_{std} - V_{td}), \tag{2.7}$$

$$\frac{dI_{stq}}{dt} = \frac{-R_{st}}{L_{st}} I_{stq} + \omega_s I_{std} + \frac{1}{L_{st}}(V_{stq} - V_{tq}). \tag{2.8}$$

2.3. **Synchronous Generator.** The block diagram of synchronous generator (SG) is shown in Fig.4(a) consists of governor, voltage controller and system stabilizer. The difference between desired and actual speed is said to be speed error, it is controlled by speed governor. Based on the difference in the speed ($\Delta\omega$), mechanical output (P_m) varies. The deviation in terminal voltage (ΔV_t) is derived from the difference of P_m with ΔP_m and P_e, where ΔP_m is disturbances in mechanical power and P_e is electric power output from generator. The transfer function of G1 is K_p $(1+\frac{1}{sT_p})$, which is used to control power deviations and also to produce voltage margin. The electric power output consists of power delivered to grid and copper and iron losses. From two space analysis, output power can be derived. Pe can also be derived from $(V_{real}I_{real}+V_{imag}I_{imag})$ and losses in electric power can be derived from $(I_{real}^2 + I_{imag}^2)R_a$, where real and imag are real and imaginary parts of voltages and current and R_a is armature resistance of SG. X_d, X_q,X_d', X_q' are direct (d) and quadrature (q) components of salient SG at steady state and at subtransient conditions. The difference in reference voltage (V_{ref}), generator terminal voltage and PSS voltage are controlled by tuning the exciter gain and time constants(K_e, T_{eo}) to get reference voltage E_f. If E_f is added with $\Delta i_d(X_q$-$X_q')$ we get E_d reference and armature quadrature component (E_q) can be obtained by multiplying $\Delta\ i_q(X_d$-$X_d')$. A first order transfer function is used to control these parameters so as to get voltages $\Delta V_d'$ and $\Delta V_q'$.The final output voltage from armature of synchronous voltage (V_a) can be obtained from $\sqrt{\Delta V_d' + \Delta V_q'}$. This voltage has to be maintained at desired values to maintain synchronism with grid and other synchronous generators. The reference voltage (V_{ref} or $\Delta\ V_{ref}$) is obtained from grid potential transformer and stabilizer voltage (V_s or ΔV_s) are obtained from PSS. The most widely used lead-lag controller design for PSS is shown in Fig.4(a). Here ω_0 is fundamental angular frequency which is equal to 2πf, where f is frequency of the generator.

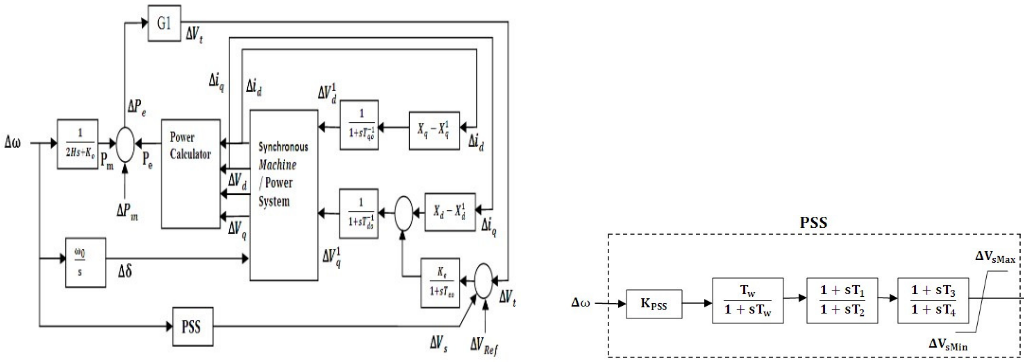

(a) Synchronous generator with PSS

(b) 5^{th} order PSS with speed

FIGURE 4. Synchronous generator and PSS

2.4. **Power system stabilizer (PSS).** The block diagram representation of 5^{th} order PSS is shown in Fig.4(b). If a disturbance occurs to power system, if the system regains its pre-disturbance state is defined as stable. During or after disturbance, oscillations in generator parameters take place and if these oscillations are damped quickly then system comes to steady state operation. For oscillations damping PSS is used. Kpss is PSS gain constant; Tw is washout time constant, its value is about 30 seconds [10]. Lower than this value oscillations persist. T_1 and T_3 are lead time constants and T_2 and T_4 are lag time constants of the signal generator. For compensating excitation control system and also to maintain local phase lag, lead time constants are to be tuned and to improve stability lag time constants are used. From stability studies like Eigen or Root Locus, it is observed that T_2 and T_4 values must be made smaller than T_1 and T_3. For active power oscillations damping,

$$\frac{2HS_B}{\omega_0}\frac{d\omega_s}{dt} = P_{turbine} - P_{ref} - K(\omega_l - \omega_0). \tag{2.9}$$

The above equation is very commonly used to explain the state of system for synchronous generator. For machine to reach equilibrium $\frac{\Delta\omega_l}{dt}$ should be equal to zero. It is achieved when $P_{turbine}$= P_{ref} and ω_s=ω_l=ω_0 where ω_l is measured from AC lines using phase locked loop (PLL).

3. Block diagram of H∞ controller

The H∞ controller (HC) used in this paper is shown in Fig.5. The'd' represents disturbance parameter, U_1 is damping feedback component which is either frequency, real or reactive power or voltage parameters. The system or grid refers to the system under consideration which is Fig.1 in this paper. The washout filter is a conventional high-pass filter with null gain. The weighted transfer functions are W_1 and W_2 which are outputs for the HC. The weighted transfer function parameters W_1, W_2 and disturbance transfer function(d) is given by

$$W_1(s) = \left(\frac{\frac{s}{\sqrt[k]{M_s}} + w_b}{s + w_b\sqrt[k]{\zeta}}\right)^k \quad \text{and} \quad W_2(s) = \left(\frac{s + \frac{w_{bc}}{\sqrt[k]{M_n}}}{\sqrt[k]{\zeta_1}s + w_{bc}}\right)^k$$

$$\text{with} \quad d = \left(\frac{\omega^2}{s^2 + 2\zeta\omega s + \omega^2}\right).$$

The two weighted transfer functions parameters and coefficients are w_b , w_bc are bandwidths, M_s, M_n are peak sensitivity, ζ, ζ_1 are steady state errors, K is the order of the transfer function and damping ratio ζ operates in the region of $\cos(\frac{\theta}{2})$ which operates in the left half of the complex plane. U1 is the step change in the magnitude.

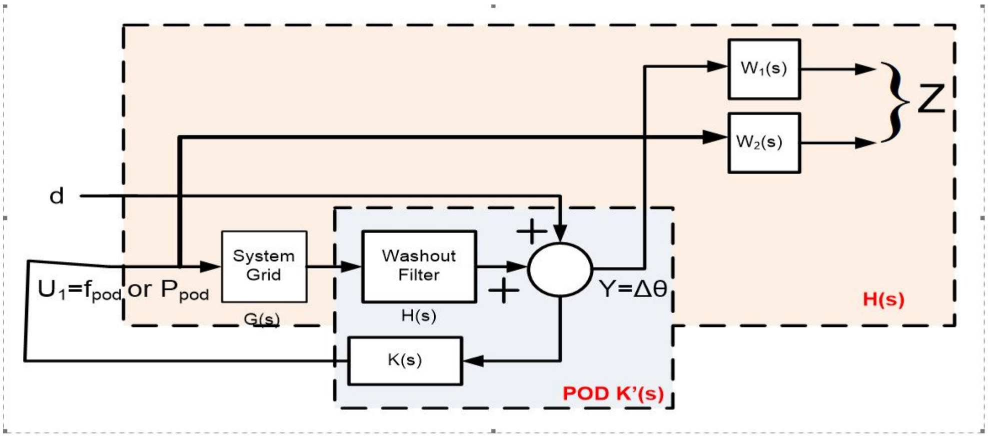

FIGURE 5. Block Diagram of H∞ controller

4. RESULTS ANALYSIS

The outputs for the test system is shown in Fig.6. Here, a sudden dip in the voltage occurs at 1 second and the results of synchronous generator (SG), solar PV and STATCOM without controller (UC), with fuzzy controller (FC) and with H∞ controller (HC) is described. The analysis from top left of Fig.6 is analyzed here, also all the parameters under study are shown in per-unit (pu). The load angle of the SG in degrees is constant till 1s and slowly this angle is increasing sinusoidal as time increasing without controller (UC in red lines), this angle has an overshoot during the fault and damped effectively with FC and HC without oscillations. For this parameter, FC behavior is better than with HC as steady-state value reached quickly.

The field voltage is constant till 1s and from then uncontrolled oscillations are observed with UC, where as with FC a surge in the voltage is observed and damped in another 1s. With HC, the overshoot in the voltage is lesser and reached steady value earlier than with FC in less than a second. The rotor speed which is same as synchronous speed for the SG has no control when disturbance occurs at 1s, so it is increasing continuously and in sinusoid. The FC and HC are similar in behavior as far as speed in consideration. However, the overshoot is high for HC, but reached steady value earlier than with FC.

The solar PV cell output current is also increasing slowly in magnitude when no controller is used. This current is having positive overshoot with FC and negative overshoot with HC and the later is having more overshoot and 90%

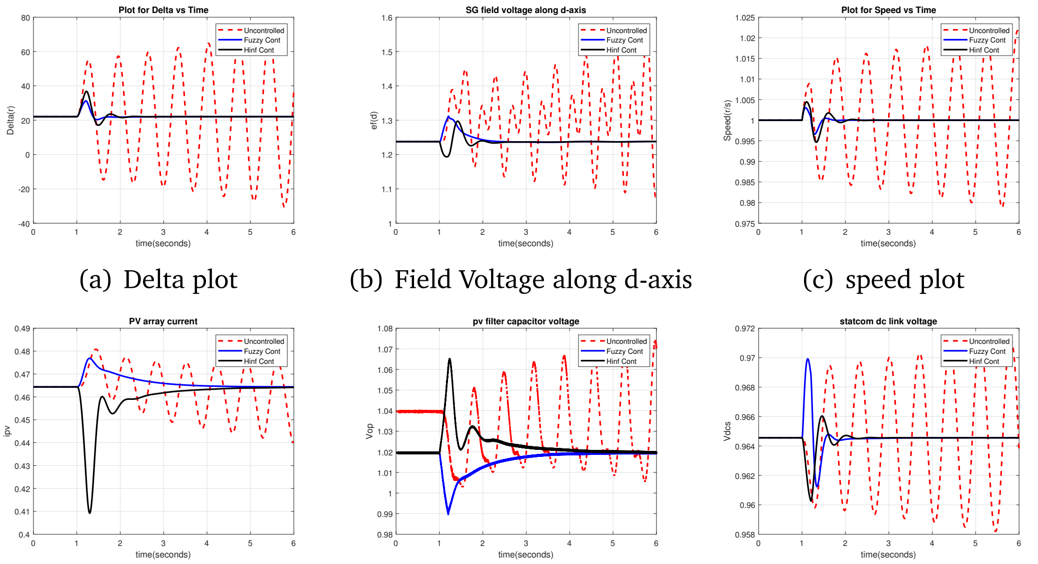

(a) Delta plot (b) Field Voltage along d-axis (c) speed plot

(d) PV current (e) PV filter capacitor voltage (f) statcom dc link voltage

FIGURE 6. Outputs of solar-PV system and STATCOM with FC and HC with disturbance at 1 second

of final value is reached quickly. Hence, HC is having better performance when PV panel control is observed. Also, the solar PV cell LCL filter voltage across the capacitor is almost same as current with UC (without controller, red color) having uncontrolled oscillations. The FC has negative overshoot and reached 90% of final value slowly than with HC which reached in less than a second.

The STATCOM dc link capacitor voltage is shown in Fig.(6). When there is no controller (UC), this voltage is also increasing continuously. With FC, there is a positive overshoot and with HC it is negative overshoot and HC is having two sustained oscillations and reached steady value quickly than with FC.

5. CONCLUSION

The H∞ controller (HC) and fuzzy controller (FC) based power oscillation damping controllers are discussed in this paper. The additional solar PV helps in meeting the additional load demand, but it has poor inertia coefficient, so STATCOM type FACTS device is used to improve the damping and indirect-inertial behavior of the solar PV panel system. It is observed that the system without controller is unable to sustain to grid voltage fault and hence resulted in unsustained oscillations in load angle delta, field voltage, rotor speed, PV panel current, PV voltage and STATCOM voltage. The same parameters are damped effectively when FC or HC is used for the same system. When compared to FC, the HC is having overshoot in the direction opposite to the synchronous generator oscillations and hence the damping effectiveness is very effective. Also, the time to reach the steady-state value quicker and lesser overshoot. The FC is not parameter dependent, but works based on the error control parameter given as an input and is based on the fuzzy membership functions. The HC is parameter dependent of the system and has very robust and effective performance.

REFERENCES

[1] KUMAR, L.V. SURESH, G.V. NAGESH KUMAR: *Power Conversion in renewable energy systems: A review advances in wind and PV system*, Inter. J. Energy Res., **41** (2017), 182–197.

[2] M. PREMKUMAR, U. SUBRAMANIAM, T.S. BABU, R.M. ELAVARASAN, L. MIHET-POPA: *Evaluation of Mathematical Model to Characterize the Performance of Conventional and Hybrid PV Array Topologies under Static and Dynamic Shading Patterns*, Energies, **13** (2020), 3216.

[3] M. PREMKUMAR, R. VIJAYA KRISHNA, R. MOHAN KUMAR, R. SOWMYA: *Protection to Grid-Tied Converters and Power Quality Control using Active Shunt Filter*, Inter. J. Engi. Adv. Tech., **8**(3) (2019), 449–456.

[4] C. LI, D. JINGCHAO, Z. XIAO-PING: *Coordinated design and application of robust damping controllers for shunt FACTS devices to enhance small-signal stability of large-scale power systems*, CSEE J. Power Energy Sys., **3**(4) (2017), 399–407.

[5] L. LUO, G. WEI, Z. XIAO-PING, C. GE, W. WEIJUN, Z. GANG, Y. DINGJUN, W. ZHI: *Optimal siting and sizing of distributed generation in distribution systems with PV solar farm utilized as STATCOM (PV-STATCOM)*, App. Energy., **210** (2018), 1092–1100

[6] M. DARABIAN, J. ABOLFAZL: *A power control strategy to improve power system stability in the presence of wind farms using FACTS devices and predictive control*, Inter. J. Electric Power Energy Sys., **85** (2017), 50–66.

[7] R.K. VARMA, M. AKBARI: *Simultaneous Fast Frequency Control and Pow-er Oscillation Damping by Utilizing PV Solar System as PV-STATCOM*, IEEE Trans. Sus. Energy, **11**(1) (2019), 415–425.

[8] S. PRASAD, P. SHUBHI, K. NAND: *H-infinity based non-linear sliding mode controller for frequency regulation in interconnected power systems with constant and time-varying delays*, IET Gen. Trans. Distri., **10**(11) (2016), 2771–2784.

[9] KUMAR, L.V. SURESH, G.V. NAGESH KUMAR, S. MADICHETTY: *Pattern search algorithm based automatic online parameter estimation for AGC with effects of wind power,* Inter. J. Electric Power Energy Sys., **84** (2017), 135–142.

[10] D.V.N. ANANTH, G.V. NAGESH KUMAR: *Mitigation of voltage dip and power system oscillations damping using dual STATCOM for grid connected DFIG,* Ain. Shams. Engi. J., **8**(4) (2017), 581–592.

DEPARTMENT OF ELECTRICAL AND ELECTRONICS ENGINEERING
GMR INSTITUTE OF TECHNOLOGY
RAJAM, ANDHRA PRADESH, INDIA
Email address: lvenkatasureshkumar@gmail.com,sureshkumar.lv@gmrit.edu.in

DEPARTMENT OF ELECTRICAL AND ELECTRONICS ENGINEERING
RAGHU INSTITUTE OF TECHNOLOGY
VISAKHAPATNAM, ANDHRA PRADESH, INDIA
Email address: nagaananth@gmail.com

DEPARTMENT OF ELECTRICAL AND ELECTRONICS ENGINEERING
GMR INSTITUTE OF TECHNOLOGY
SRIKAKULAM, INDIA
Email address: mprem.me@gmail.com

SR. TRANSMISSION PLANNING ENGINEER
DUBAI ELECTRICITY & WATER AUTHORITY
DUBAI, UNITED ARAB EMIRATES
Email address: ravipudi.sudhir@dewa.gov.ae